

DOI: 10.1002/chem.201302610

## Plasmonic Scissors for Molecular Design

Mengtao Sun,<sup>\*,[a]</sup> Zhenglong Zhang,<sup>[a, b]</sup> Zee Hwan Kim,<sup>[c]</sup> Hairong Zheng,<sup>[b]</sup> and Hongxing Xu<sup>[a]</sup>

**Abstract:** Heterogeneous catalysts play an important role in surface catalytic reactions, but selective bond breaking and control of reaction products in catalytic processes remain significant challenges. High-vacuum tip-enhanced Raman spectroscopy (HV-TERS) is one of the best candidates to realize surface catalytic reactions. Herein, HV-TERS was employed in a new method to control dissociation by using hot

electrons, generated from plasmon decay, as plasmonic scissors. In this method, the N=N bond in 4,4'-dimercaptoazobenzene was selectively dissociated by plasmonic scissors, and the

**Keywords:** chemoselectivity · plasmon chemistry · radical reactions · Raman spectroscopy · surface chemistry

reaction products formed from the radical fragment (SC<sub>6</sub>H<sub>5</sub>N) were controlled by varying the pH value. Under acidic conditions, *p*-aminothiophenol was produced from the radical fragment by attachment of hydrogen ions, whereas under alkaline conditions, 4-nitrobenzenethiol was obtained by attachment of oxygen ions to the substrate.

## Introduction

Surface plasmon assisted molecular synthesis at the nanoscale is an exciting topic in the field of surface catalysis.<sup>[1–17]</sup> Recently, plasmon-assisted synthesis of 4,4'-dimercaptoazobenzene (DMAB) from *p*-aminothiophenol (PATP) and 4-nitrobenzenethiol (4NBT), revealed by surface-enhanced Raman scattering (SERS) spectroscopy, has been realized.<sup>[3,6,7]</sup> DMAB has been a subject of study for plasmon-assisted catalytic reactions,<sup>[3,5–8,10,13,16]</sup> but all of them are plasmon-assisted synthesis reactions. It is in principle possible to achieve the reverse process (dissociation) by SERS spectroscopy. Can such dissociation of DMAB be realized in SERS? However, as the hot electrons (generated from plasmon decay) required by the dissociation are mostly quenched in ambient SERS, it is desirable to find a new technique to perform the dissociation process.

High-vacuum tip-enhanced Raman spectroscopy (HV-TERS)<sup>[8,10]</sup> is among the best candidates. Nanospectroscopic resolution and spatiotemporal information from the dynam-

ic processes of single active sites have been obtained by utilizing HV-TERS.<sup>[8,11,13]</sup> The sharp metal tip in HV-TERS can create a “hot site” where strong surface plasmon resonances are excited<sup>[8,13,16–20]</sup> and, as the plasmon decays, more hot electrons are produced at the apex of the tip.<sup>[8,10]</sup> In addition, the high vacuum in HV-TERS provides substantial space in which the quenching of hot electrons is prohibited.<sup>[8]</sup> As a result, most hot electrons are effective in chemical reactions in HV-TERS. During the reactions, hot electrons are temporarily attached to molecules and charge the neutral potential-energy surface (PES) to the negative PES (PES<sup>-</sup>), thus a decrease in the reaction barrier for dissociation can be achieved.<sup>[4,8]</sup> To reveal the nature of chemical reactions assisted by hot electrons, it is important to monitor the catalytic processes of the dissociation.<sup>[2]</sup> Moreover, as the control of chemical reactions by different pH values has been realized in SERS,<sup>[21–23]</sup> it is expected that control of reaction products could also be achieved by varying the pH value in HV-TERS.

Herein, we present selective bond breaking of DMAB by using hot electrons as plasmonic scissors and, in particular, the control of the dissociation products by varying the pH value. The N=N bond of the DMAB molecule was selectively dissociated by plasmonic scissors, PATP was produced from the radical fragment through hydrogen-ion attachment under acidic condition, and 4NBT was obtained by attachment of oxygen ions to the substrate under alkaline condition. A schematic of the home-made HV-TERS based on a scanning tunneling microscope (STM), the dissociation mechanism, and product control are shown in Figure 1.

[a] Prof. M. Sun, Dr. Z. Zhang, Prof. H. Xu  
Beijing National Laboratory for Condensed Matter Physics  
Institute of Physics, Chinese Academy of Sciences  
P. O. Box 603-146, Beijing, 100190 (P. R. China)  
E-mail: mtsun@iphy.ac.cn

[b] Dr. Z. Zhang, Prof. H. Zheng  
School of Physics and Information Technology  
Shaanxi Normal University  
Xi'an, 710062 (P. R. China)

[c] Prof. Z. H. Kim  
Department of Chemistry, Korea University  
Seoul 136-701 (Korea)

Supporting information for this article is available on the WWW under <http://dx.doi.org/10.1002/chem.201302610>.

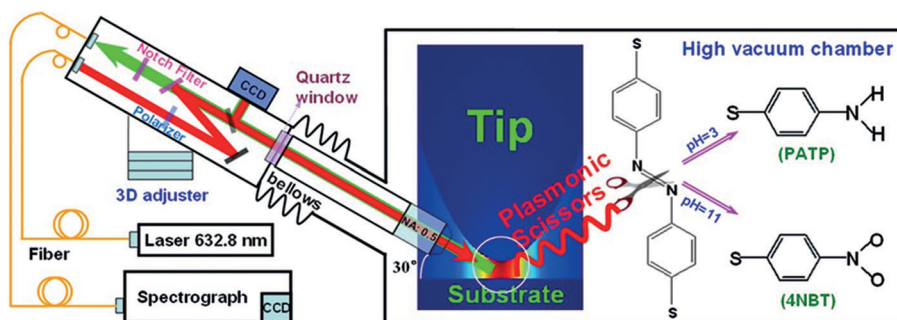


Figure 1. Schematic of HV-TERS, mechanism of dissociation by plasmonic scissors and the product control by means of different pH values.

## Results and Discussion

Figure 2a shows the TER spectrum of DMAB adsorbed on Ag film. It is the same as the normal Raman spectrum (NRS) of DMAB powder shown in Figure 2b. Theoretical

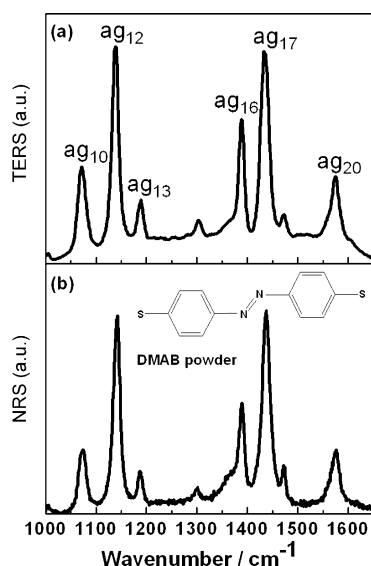


Figure 2. TER and NR spectra of DMAB. a) TER spectrum of DMAB adsorbed on Ag film at tunneling current of 1 nA and bias voltage of 1 V. b) NRS of DMAB powder. The excitation wavelength was 632.8 nm.

assignments of these vibrational modes can be found in reference [3]. The  $ag_{17}$  vibrational mode ( $1433\text{ cm}^{-1}$ ) of DMAB corresponds to the N=N stretching mode. This peak in the TER spectrum decreased, or even disappeared, when DMAB was selectively dissociated by plasmonic scissors. We tried to detect the signals of the dissociation by continuous radiation, but the TER spectra stayed the same as shown in Figure 2a. Time-sequential spectral analysis also did not reveal any change. According to our previous works on the molecular synthesis of DMAB from PATP and 4BNT, the dissociated fragments dimerize back to DMAB very quickly through the N=N bond. Clearly, the dissociation cannot be observed in a competing process between dissociation and synthesis,<sup>[7]</sup> and new avenues are required.

To prevent the dissociated radical fragments from dimerization, we manipulated the pH values to control the reaction paths in HV-TERS. Under acidic conditions, DMAB in the nanogap was firstly excited by 100% laser (2 mW), and TER spectra were measured in the time span from 0 to 60 min. If the N=N bond of DMAB in the tip/molecule/substrate system is selectively broken, then the dissociated fragments will be located on the tip and substrate, respectively. As shown in Figure 3a and b, no significant change could be obtained by strong excitation for 60 min. Then we retracted the substrate and applied 1% laser (20  $\mu$ W) radiation on the in situ apex of the tip. Figure 3c

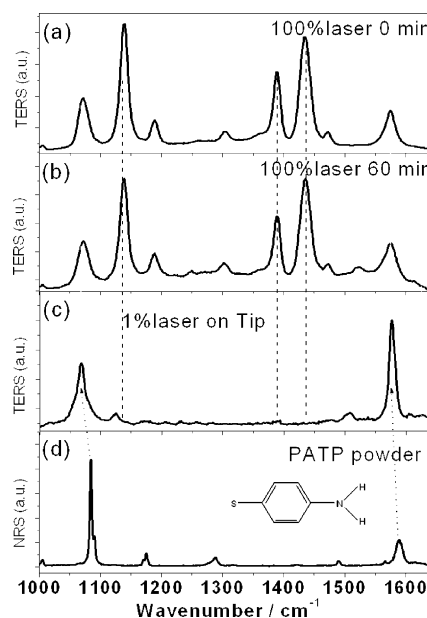


Figure 3. Experimental TER (acidic conditions) and NR spectra. TER spectra of DMAB at a) 0 and b) 60 min. c) TER spectrum on tip with weak excitation after strong excitation for 60 min. d) NRS of PATP powder.

shows the measured TER spectrum on the tip with weak plasmon intensity, which is significantly different from Figure 3a. The complete disappearance of the  $ag_{17}$  mode of DMAB in Figure 3c revealed that the N=N bond of DMAB was selectively dissociated. After this dissociation, it is proposed that the radical fragments will be converted to PATP by the attachment of hydrogen ions due to the abundant hydrogen ions adsorbed on the substrate under acidic conditions. To confirm the above assumption, we measured the NRS of PATP powder (Figure 3d). The similarity between Figure 3c and Figure 3d suggests that, in the nanogap be-

tween tip and substrate, PATP was converted to DMAB again and thus could not be detected in the nanogap. It has been shown that PATP can not be converted to DMAB easily at low plasmon intensity below the reaction threshold.<sup>[24]</sup> Our previous experimental and theoretical studies revealed the SER spectrum of PATP, in which the NH vibrational peak around  $1610\text{ cm}^{-1}$  is weak and very close to the vibrational mode of the phenyl ring at  $1586\text{ cm}^{-1}$ . Hence, the NH vibrational mode is hard to observe experimentally.<sup>[24]</sup> In fact, the symmetric and asymmetric NH vibrational modes around  $1610\text{ cm}^{-1}$  can be observed, though they are very weak. The TER spectrum of PATP in Figure 3c is similar to Figure 2b in reference [24].

We also measured TER spectra of DMAB under alkaline conditions. Figure 4a–c show the spectra collected at 0, 10, and 60 min, respectively. The vibrational peak at  $1336\text{ cm}^{-1}$  appears weakly in Figure 4b after 100% laser excitation for 10 min. The vibrational peak at  $1336\text{ cm}^{-1}$  had obviously increased at 60 min with a decrease in the vibrational peak at  $1433\text{ cm}^{-1}$  for the N=N stretching mode of DMAB (Figure 4c). After 100% laser excitation for 60 min, we retracted the substrate and applied 1% laser radiation to the in situ apex of the tip. Figure 4d shows the TER spectrum measured on the tip with 1% laser intensity, which was significantly different from Figure 4a. The vibrational peak at  $1433\text{ cm}^{-1}$  almost disappeared and only three Raman peaks were obtained in Figure 4d, which is similar to the NRS of 4NBT powder in Figure 4e. It was therefore proposed that the dissociated radical fragments were converted to 4NBT by oxygen-ion attachment due to the abundant oxygen ions adsorbed on the substrate under alkaline conditions. The TER spectrum of 4NBT in Figure 4c is similar to Figure 3c in reference [6], though the Raman intensity of the  $\text{NO}_2$  stretching mode of 4NBT at  $1336\text{ cm}^{-1}$  is not strong enough.

The physical origins of the pH-controlled products in the dissociation by plasmonic scissors in HV-TERS can be summarized in the steps shown in Figure 5. Firstly, hot electrons generated by plasmon decay are attached temporarily to the PES of DMAB, which charges the PES to  $\text{PES}^-$  and decreases the reaction barrier. Secondly, the reaction energy can be excited to be higher than or close

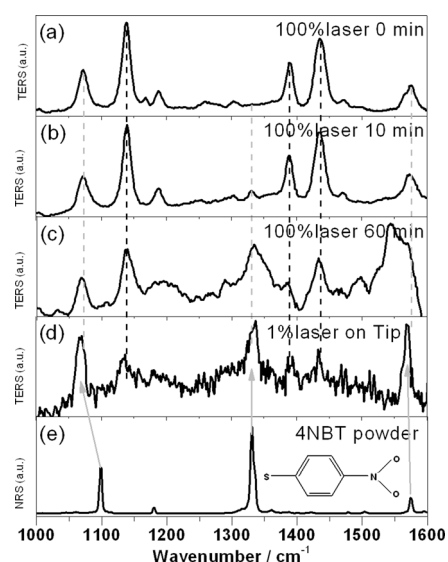


Figure 4. Experimental TER (alkaline conditions) and NR spectra. TER spectra of DMAB at a) 0, b) 10, and c) 60 min. d) TER spectrum on tip with weak excitation after strong excitation for 60 min. e) NRS of 4NBT powder.

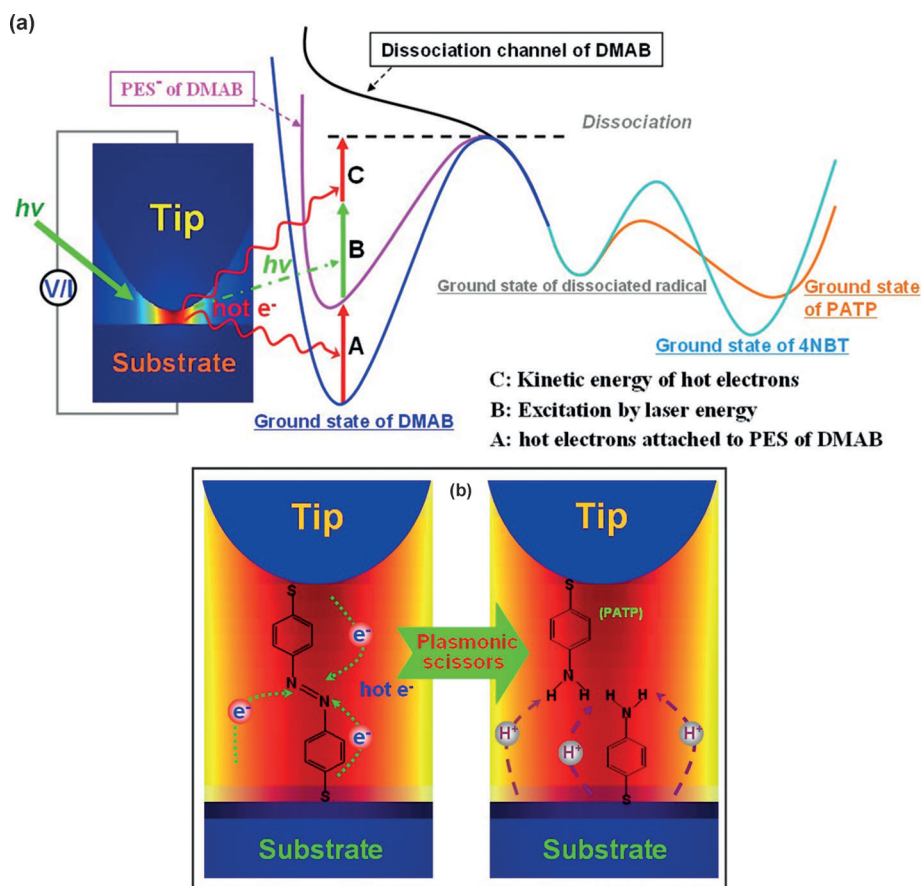


Figure 5. The process of pH control of products of the dissociation by plasmonic scissors in HV-TERS. a) Scheme of reaction paths, in accordance with experimental results. b) Dynamic process of chemical reaction under acidic conditions.

to the dissociation energy by laser. This is consistent with reference [4]. Then, the high kinetic energy of the hot electrons provides the additional energy required for selective dissociation of the N=N bond in DMAB. This is consistent with reference [12]. Lastly, the dissociated radicals absorb hydrogen or oxygen ions on the substrate under acidic or alkaline conditions, respectively. By this mechanism, PATP or 4NBT is produced through their individual reaction paths controlled by the pH value.

In general, the reaction products PATP and 4NBT can return to DMAB if enough energy is provided that the potential barrier is overcome. Both the reaction products and DMAB could exist in the reaction process at the same time. Under our experimental conditions, the reaction barriers to PATP (or 4NBT) from the ground state of the dissociated radical are lower than the reaction barrier back to DMAB, so pH-controlled PATP and 4NBT can be successfully observed experimentally. Furthermore, PATP has a lower potential barrier and faster reaction rate than 4NBT, and PATP has a faster reaction rate and needs less energy to react. Since 4NBT has a higher potential barrier than PATP, the reaction is then more difficult and slower, which explains why the dynamics of the reaction process could only be obtained under alkaline conditions (see Figures 3 and 4).

According to the above analysis and findings, to selectively dissociate DMBA through the N=N bond and to obtain stable signals from the dissociation products, three conditions are necessary. Firstly, strong and continuous plasmonic scissors must be generated from strong surface plasmons; secondly, attachment of hydrogen or oxygen ions is needed for production stable products, which provides a lower reaction barrier; lastly, to avoid triggering the backwards synthetic process, weak plasmons are needed to collect the Raman signals from the products. HV-TERS has the advantages that the high vacuum provides a favorable environment for surface plasmons and the plasmon intensity is easily manipulated by means of the laser intensity, tunneling current, and bias voltage. Therefore, the pH-control of products in the dissociation by plasmonic scissors can be successfully realized in HV-TERS.

The N=N bond of *trans*-azobenzene is very strong, with a bond dissociation energy of 4.04 eV (390 kJ mol<sup>-1</sup>).<sup>[25]</sup> Li and Diebold found that a rutile TiO<sub>2</sub> (110) crystal surface is capable of breaking the rather strong N=N double bond of *trans*-azobenzene to give an organized structure of phenyl imide fragments.<sup>[26]</sup> The calculated dissociation energy of the *trans*-azobenzene molecule adsorbed on TiO<sub>2</sub> (110) is significantly decreased, to 2.73 eV.<sup>[27]</sup> In our experiment, the laser energy for the plasmon-assisted dissociation of N=N bond of DMAB is 633 nm (1.959 eV), which represents a further decrease in dissociation energy. Thus, the reaction barrier is significantly lower in plasmon-driven dissociation, and product manipulation is feasible by controlling the experimental conditions.

It was reported that near-infrared continuous-wave light can drive two-photon chemical reactions with the assistance of localized surface plasmons.<sup>[17]</sup> The incoherent inelastic

scattering of two photons on the vibrational quantum states is called hyper Raman scattering (HRS). HRS results in Raman signals shifted relative to the second harmonic of the excitation laser. Tip-enhanced hyper Raman scattering (TEHRS) can change the parity and thus break the selection rules. In addition, not only the a<sub>g</sub> but also the b<sub>u</sub> modes should be observed experimentally by TEHRS. In our experiments, only the a<sub>g</sub> mode of reagent molecules was observed. Thus, the mechanism of continuous-wave light-driven two-photon chemical reaction with the assistance of localized surface plasmons can be excluded in our experiment.

## Conclusion

We have presented selective bond breaking of DMAB by hot electrons acting as plasmonic scissors. The dissociation products can be controlled by means of the pH value: PATP was produced from the radical fragment by hydrogen-ion attachment under acidic conditions, while 4NBT was obtained by the attachment of oxygen ions under alkaline conditions. The physical mechanisms of bond-selective dissociation and pH controlled products were rationally interpreted.

## Experimental Section

4,4'-Dimercaptoazobenzene (4,4'-DMAB, *M*<sub>r</sub> = 246.4) was custom-synthesized by Medigen Co. and delivered as a light yellow solid. The parent mass peak (*m/z*) corresponding to the protonated form of the compound was identified at 247.3 ([*M*+H]<sup>+</sup>), and three signals were identified in the <sup>1</sup>H NMR spectrum at 3.6 for SH, 7.4 for 2-CH, and 7.8 ppm for 3-CH (see the Supporting Information).

The TER spectra were measured with a home-built HV-TERS setup, as shown in Figure 1. It consists of an STM in a high-vacuum chamber, a Raman spectrometer with side illumination of 632.8 nm He-Ne laser light with an angle of 60° to the tip axis for Raman measurements and three-dimensional piezo stages for the tip and sample manipulations. The pressure in the vacuum chamber is about 10<sup>-7</sup> Pa. A gold tip with the diameter of about 50 nm was made by electrochemical etching of a 0.25 mm-diameter gold wire.<sup>[28]</sup> The substrate was prepared by evaporating a 100 nm silver film onto a freshly cleaned mica film under high vacuum. In the Au tip/Au substrate system, IR vibrational modes of DMAB were also active,<sup>[10,29]</sup> so for simplification of our study we chose Ag as substrate. The film was immersed in a 1 × 10<sup>-5</sup> M ethanolic solution of DMAB at pH values of 3, 7, and 11 for 4 h and then rinsed with ethanol for 10 min to guarantee that there was only one monolayer of 4NBT molecules adsorbed on the silver film. Then the sample was immediately put into the high-vacuum chamber. To get a good signal-to-noise ratio, the TERS signals were collected with an acquisition time of 20 s and accumulated ten times (exception: one time for Figure 4d). The NRS of PATP, 4NBT, and DMAB powders were measured by using Leica microscopy equipment in a confocal Raman spectroscopic system (Renishaw, Invia), and the incident wavelength was 632.8 nm.

## Acknowledgements

This work was supported by the National Natural Science Foundation of China (Grants 11374353, 11274149, and 11174190), the National Basic

Research Project of China (Grants 2009CB930701), the Program of Shenyang Key Laboratory of Optoelectronic Materials and Technology (Grant No. F12-254-1-00), and the Fundamental Research Funds for the Central Universities (GK201101006).

- [1] C. J. Chen, R. M. Osgood, *Phys. Rev. Lett.* **1983**, *50*, 1705.  
 [2] D. R. Killelea, V. L. Campbell, N. S. Shuman, *Science* **2008**, *319*, 790.  
 [3] Y. R. Fang, Y. Z. Li, H. X. Xu, M. T. Sun, *Langmuir* **2010**, *26*, 7737.  
 [4] P. Christopher, H. Xin, S. Linic, *Nat. Chem.* **2011**, *3*, 467.  
 [5] H. Choi, H. K. Shon, H. Yu, T. G. Lee, Z. H. Kim, *J. Phys. Chem. Lett.* **2013**, *4*, 1079.  
 [6] B. Dong, Y. R. Fang, X. W. Chen, H. X. Xu, M. T. Sun, *Langmuir* **2011**, *27*, 10677.  
 [7] T. Sun, H. X. Xu, *Small* **2012**, *8*, 2777.  
 [8] M. T. Sun, Z. L. Zhang, H. R. Zheng, H. X. Xu, *Sci. Rep.* **2012**, *49*, 647.  
 [9] K. D. Watanabe, N. Menzel Nilius, H. Freund, *Chem. Rev.* **2006**, *106*, 4301.  
 [10] M. T. Sun, Y. R. Fang, Z. Y. Zhang, H. X. Xu, *Phys. Rev. E* **2013**, *87*, 020401.  
 [11] H. Kim, K. M. Kosuda, R. P. Van Duyne, P. C. Stair, *Chem. Soc. Rev.* **2010**, *39*, 4820.  
 [12] S. Gao, K. Ueno, H. Misawa, *Acc. Chem. Res.* **2011**, *44*, 251.  
 [13] M. van Schroyen Lantman, T. Deckert-Gaudig, A. J. G. Mank, V. Deckert, B. M. Weckhuysen, *Nat. Nanotechnol.* **2012**, *7*, 583.  
 [14] W. Xu, J. S. Kong, Y-T. E. P. Yeh, Chen, *Nat. Mater.* **2008**, *7*, 992.  
 [15] C. Novo, A. M. Funston, P. Mulvaney, *Nat. Nanotechnol.* **2008**, *3*, 598.  
 [16] W. Xie, B. Walkenfort, S. Schlucher, *J. Am. Chem. Soc.* **2013**, *135*, 1657.  
 [17] Y. Tsuboi, R. Shimizu, T. Shoji, N. Kitamura, *J. Am. Chem. Soc.* **2009**, *131*, 12623.  
 [18] R. M. Stöckle, S. Y. Doug, V. Deckert, R. Zenobi, *Chem. Phys. Lett.* **2000**, *318*, 131.  
 [19] N. Hayazawa, Y. Inouye, Z. Sekkat, S. Kawata, *Opt. Commun.* **2000**, *183*, 333.  
 [20] M. Sun, Z. Zhang, L. Chen, H. Xu, *Adv. Opt. Mater.* **2013**, *1*, 449.  
 [21] A. Pallaoro, G. B. Braun, N. O. Reich, M. Moskovits, *Small* **2010**, *6*, 618.  
 [22] M. Sun, Y. Huang, L. Xia, X. Chen, H. Xu, *J. Phys. Chem. C* **2011**, *115*, 9629.  
 [23] S. Zong, Z. Wang, J. Yang, Y. Cui, *Anal. Chem.* **2011**, *83*, 4178.  
 [24] X. Tian, L. Chen, H. Xu, M. Sun, *RSC Adv.* **2012**, *2*, 8289.  
 [25] M. F. Budyka, M. M. Kantor, *Russ. Chem. Bull.* **1993**, *42*, 1495.  
 [26] S. C. Li, U. Diebold, *J. Am. Chem. Soc.* **2010**, *132*, 64.  
 [27] J. P. Prates Ramalho, F. Illas, *Chem. Phys. Lett.* **2011**, *501*, 379.  
 [28] B. Ren, G. Picardi, B. Pettinger, *Rev. Sci. Instrum.* **2004**, *75*, 837.  
 [29] Z. Zhang, M. Sun, P. Ruan, H. Zheng, H. Xu, *Nanoscale* **2013**, *5*, 4151.

Received: July 5, 2013

Revised: July 28, 2013

Published online: September 13, 2013